

Enhancement of the anti-corrosion performance based on the zeolitic imidazolate framework

J. W. Shen, X. Z. Fang*, Z. W. Feng, X. Huang

*School of Materials Engineering, Jiangsu University of Technology, Changzhou
213001, China*

In this work, a zeolite-imidazole framework (ZIF-8) was first synthesized and used as a corrosion inhibitor container to enhance the anti-corrosion property. After encapsulated the benzotriazole (BTA) corrosion inhibitor and coated with epoxy resin (EP) on the surface of Cu plate, the obtained sample B-ZIF-8@EP exhibited enhanced corrosion protection with high impedance and positive self-corrosion potential due to the release of BTA in the corrosion process. It is believed that this work is very helpful for extending the diversity of anti-corrosion coatings.

(Received December 12, 2023; Accepted March 8, 2024)

Keywords: ZIF-8, Anti-corrosion property, Epoxy resin

1. Introduction

Metal is one of the most widely used materials in marine industry, aerospace, transportation, construction, energy and other fields among the world^[1]. However, due to the active property and complex environments during long-term service, the metal is prone to corrode and loss the efficacy. The corrosion of metal has caused serious environmental pollution and huge economic losses as well as significant security accidents^[2]. Therefore, the metal protection is an urgent demand with the growing usage. Conventional anti-corrosion technologies include optimized metal structure^[3], polymeric coating^[4-7], electrochemical protection^[8], and corrosion inhibitor^[9-11]. Among the various anti-corrosion technologies, polymeric coatings are one of the effective method due to the good stability in acidic/alkaline conditions, excellent adhesion, high mechanical properties, low cost, and so on^[5]. However, in the long-term service exposed in a harsh environment, polymeric coating are susceptible to the permeation of corrosive ions (chloride ions, oxygen, or water molecules) due to the micropores and cracks (created during the curing reactions of coatings or exposure to outdoor). Followed, the corrosive ions prefer to concentrate in the micropores and cracks and form the corrosion micro-batteries, leading to the electrochemical corrosion occurs on the substrate^[12]. Eventually, the polymeric coating loses its protection and the corrosive metal loses the practicability. Therefore, it is a huge challenge to solve the problems about corrosion when micropores and cracks appeared in the polymeric coating.

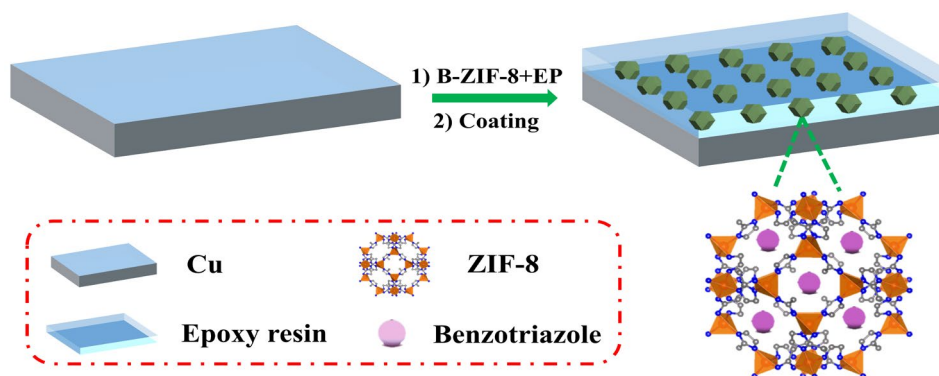
* Corresponding author: 2017500077@jsut.edu.cn

<https://doi.org/10.15251/DJNB.2024.191.401>

The smart polymeric coatings with superior self-healing anti-corrosion activity will be a good strategy to overcome this problem. During the construction of smart coatings, the employment nanocontainers or nanocapsules capable of absorption and desorption of active inhibitors will enhance the coating compactness and self-healing capacity^[13,14]. The most important micro and nanocontainers used in anti-corrosion applications are the halloysite nanotubes, mesoporous TiO₂, mesoporous silica, and carbon-based materials like graphene oxide (GO) and carbon nanotube^[13,14]. However, recent years have seen increased interest in the new nanocontainer-metal organic frameworks (MOFs), which is an ideal candidate due to the high pore volume, hydrophobicity and thermal stability^[15,16].

MOFs, constructed by organic linker and metallic precursor, is a relatively new porous materials. Due to the diversity of organic linker and metallic precursor, the structure of MOFs is various and tunable, leading to changes in the frameworks (pore size, surface area, stability, and so on)^[17]. Making use of such properties, MOFs has been widely applied in different fields, such as gas storage and separation, sensors, catalysts, drug delivery, heat transformation, CO₂ sorption, and so on^[18]. Recently, in the metal protection, the MOFs has drawn the focus of researchers in the construction of polymeric coatings to provide anti-corrosion or active protection properties^[19-21]. The MOFs itself in polymeric coatings can serve as the nanocontainer to load corrosion inhibitors or as a corrosion barrier. At the same time, the structure of some MOFs is sensitive to the stimulus, such as pH alterations, humidity, temperature, irradiation, and so on, which can be used in the smart polymeric coatings.

Inspired by the foregoing, a representative type of MOFs, zeolite-imidazole framework (ZIF-8) was chosen as the nanocontainer to build the polymeric coating^[22]. Construct by the 2-methylimidazole and Zinc ions, the ZIF-8 possesses a porous structure with the cavity and aperture around 11.6 Å and 3.4 Å, respectively. Meantime, the structure of ZIF-8 is analogous to the silicon-based zeolites, having some advantage of zeolites but better compatibility with coatings than zeolites. Furthermore, the ZIF-8 is sensitive to the pH alterations, which can be served as the smart switch to release the inhibitor^[23]. Hence, as illustrated in Scheme 1, through the modification, benzotriazole (BTA) as corrosion inhibitor and self-healing agent was encapsulated into ZIF-8 nanocontainer (denoted as B-ZIF-8). Subsequently, the as-synthesized B-ZIF-8 was used to construct the epoxy resin (EP) coating (denoted as B-ZIF-8@EP)^[24]. After a series of characterizations and tests, the as prepared B-ZIF-8@EP enhances the anti-corrosion abilities due to the self-healing property of BTA release.



Scheme 1. Schematic illustration showing the synthesis of B-ZIF-8@EP for the enhanced corrosion protection.

2. Experimental

2.1. Materials

All chemicals were obtained from commercial suppliers in China without any further purification. Zinc nitrate hexahydrate ($\text{Zn}(\text{NO}_3)_2 \cdot 6\text{H}_2\text{O}$), 2-Methylimidazole, and benzotriazole (BTA) were obtained from Aladdin Chemical Reagent Co., Ltd.. Copper foil was purchased from Anping Tairun Wire Mesh Co., Ltd.. Epoxy resin (E 51) were purchased from Shanghai Chemical Reagent Co., Ltd..

2.2. Method for preparing coatings containing B-ZIF-8

ZIF-8 was synthesized according to the reported literature with some modification. Typically, Zinc nitrate hexahydrate (1.68 g) and 2-Methylimidazole (3.70 g) were dissolved in methanol, respectively. Mixing the solution and stirring for 24 h under room temperature, white crystals were obtained. Through centrifugation, wash with methanol and then dry in a vacuum oven overnight, the ZIF-8 was obtained.

ZIF-8 (100 mg) and BTA (100 mg) were dissolved in 20 mL methanol and stirred for 24 h under room temperature. Followed, the mixture was put into vacuum oven under negative pressure state at room temperature to encapsulate the BTA into ZIF-8. The sample was then washed with ethanol several times to remove redundant substance and dried at 40 °C in to obtain the B-ZIF-8 sample.

B-ZIF-8 (50 mg) was dispersed in 8 g epoxy resin and stirred for 20 min to ensure the uniform dispersion. Then 2 g curing agent was added and stirred for 20 min to fully dispersed. Followed, the sample was placed into vacuum oven under negative pressure state for 10 min at room temperature and then deposited on the Cu plate via spraying technology and cured for 24 h at room temperature. The coating containing the B-ZIF-8 (denoted as B-ZIF-8@EP) was obtained. For comparison, the coating containing ZIF-8 (denoted as ZIF-8@EP) was also obtained with the same method using ZIF-8 instead of the B-ZIF-8.

3. Results and discussion

In the synthetic process of B-ZIF-8 sample, the ZIF-8 was first obtained. The XRD was used to confirm the crystalline phases of the prepared ZIF-8. As shown in Figure 1a, all peaks of the as-synthetic ZIF-8 are well matched with those of the simulated ZIF-8, indicating the successfully synthesis of ZIF-8. Next, through incorporating the benzotriazole inhibitor into the frameworks, the B-ZIF-8 sample was obtained. After confirmed with XRD, the peaks of ZIF-8 remains unchanged, indicating the structure is not destroyed after the post-synthesis. Furthermore, the infrared absorption spectroscopy was used to confirm the chemical structure of these samples. As shown in Figure 1b, the FT-IR spectra of ZIF-8 and B-ZIF-8 are almost similar, indicating that they own similar functional groups. However, in the spectra of B-ZIF-8, there are some new absorption peaks appeared around 751, 927, 1105.5 and 1266.5 cm^{-1} . Compared with BTA, all those new peaks are attributed to the vibration of chemical structure of BTA, indicating the successful encapsulation in ZIF-8 channels.

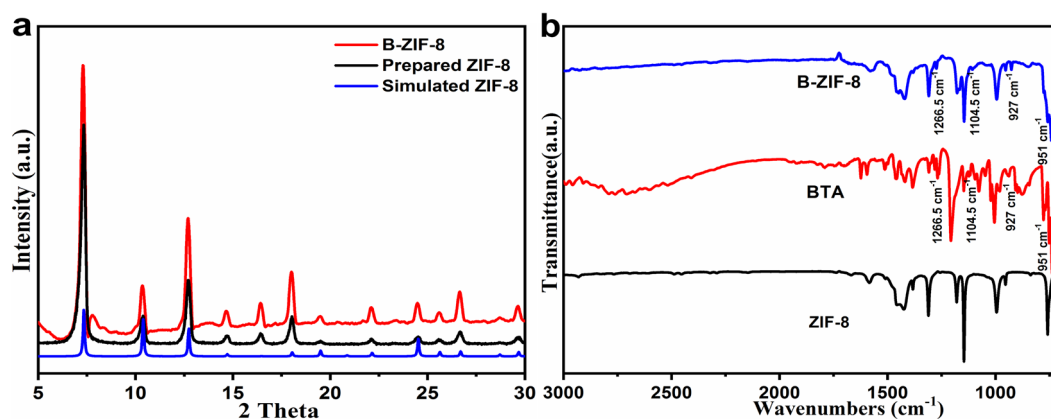


Fig. 1. (a) XRD pattern for the prepared ZIF-8. (b) FT-IR spectra for BTA, ZIF-8 and B-ZIF-8.

The morphology of ZIF-8 and B-ZIF-8 were also investigated through the SEM. As shown in Figure 2a, regular size ZIF-8 nanoparticles are obtained with the 100 nm diameter. After post-synthesis, the morphology of B-ZIF-8 nanoparticles are not exhibited obvious change, indicating the BTA is not affected the morphology of ZIF-8.

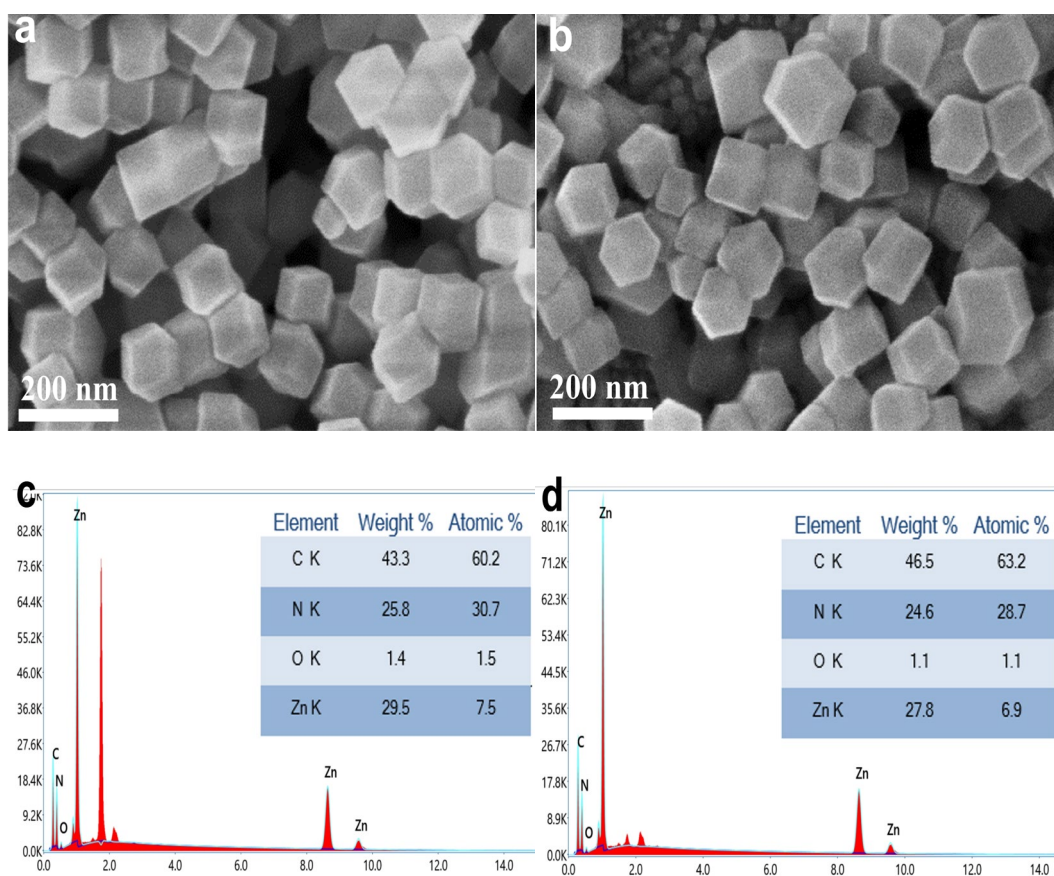


Fig. 2. SEM image for (a) ZIF-8 and (b) B-ZIF-8. The energy dispersive spectrometer (EDS) for (c) ZIF-8 and (d) B-ZIF-8.

Furthermore, the energy dispersive spectrometer (EDS) was used to analyze the element of the samples. As expected in Figure 2, the C, N, O and Zn elements are detected in the ZIF-8 and B-ZIF-8. Due to the nitrogen content of BTA is lower than that of ZIF-8, the content of N element in composite material B-ZIF-8 is lower than that of ZIF-8. For comparison, the contents of C element is increased and the total content of Zn and O element is decreased, further demonstrating the successful encapsulation of BTA into ZIF-8, which is consistent with the result of XRD and FT-IR spectra.

In order to explore the anti-corrosive property, the polarization curves of B-ZIF-8@EP, ZIF-8@EP and bare metal coated with EP were measured in the 3.5 wt% NaCl solution. The data are shown in Figure 3. Through fitting, it can be concluded that the self-corrosion current for B-ZIF-8@EP, ZIF-8@EP and bare metal are 0.76, 0.77 and 0.77 A/cm², respectively. The similar self-corrosion current indicate that under the test condition, the samples exhibit similar anti-corrosive ability. However, self-corrosion potential of the three samples were different from the polarization curves. The B-ZIF-8@EP shows the most positive self-corrosion potential of -0.38 V and the bare metal with EP shows the most negative self-corrosion potential of -0.59 V, indicating the B-ZIF-8@EP possess the best anti-corrosive ability than ZIF-8@EP and bare metal. Furthermore, the EIS was used to explore the good anti-corrosion of B-ZIF-8@EP. As illustrated in Figure 3b, the B-ZIF-8@EP exhibits the highest impedance than others, meaning that under the same self-corrosion potential, the B-ZIF-8@EP can be lost the minimum electrons due to the high resistance. The polarization curves and the EIS results indicate that the B-ZIF-8 can efficiently enhance the impedance, thus enhance the anti-corrosive property.

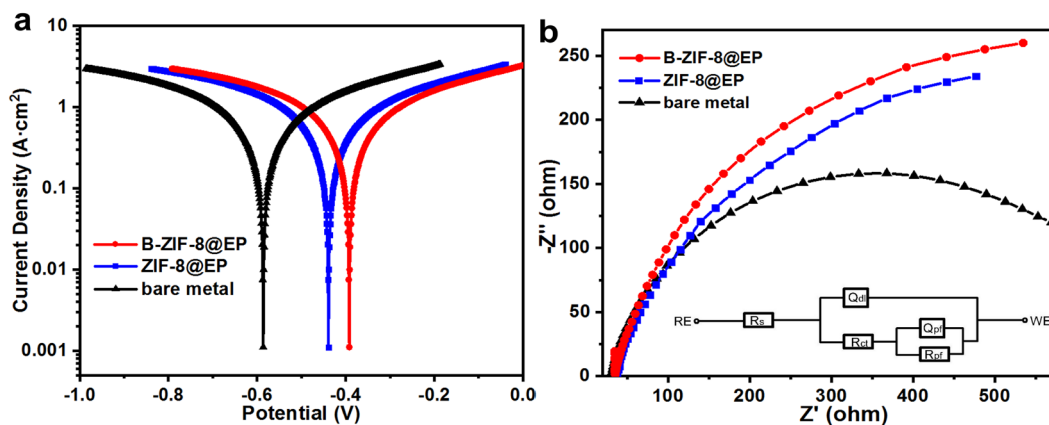


Fig. 3. (a) The potentiodynamic polarization curves of bare metal, ZIF-8@EP and B-ZIF-8@EP. (b) The Nyquist diagrams and equivalent electrical circuit of bare metal, ZIF-8@EP and B-ZIF-8@EP.

In conclusion, the corrosion inhibitor benzotriazole was successfully encapsulated into the channel of ZIF-8. After mixed with the EP and coated on the Cu metal, the obtained B-ZIF-8@EP exhibited high impedance and excellent corrosion protection ability due to the release of benzotriazole into the interface. Therefore, the B-ZIF-8@EP has shown promising potential as corrosion-inhibiting coatings for metals in service.

References

- [1] Zhao Z, Bai P, Misra RDK, et al., *Journal of Alloys and Compounds*, 792 (2019) 203-214; <https://doi.org/10.1016/j.jallcom.2019.04.007>
- [2] M.J. Anjum, J. Zhao, V. Zahedi Asl, et al., *Corrosion Science*, 157 (2019) 1-10; <https://doi.org/10.1016/j.corsci.2019.05.022>
- [3] B. Jiang, Q. Xiang, et al., *Corrosion Science*, 126 (2017) 374-380; <https://doi.org/10.1016/j.corsci.2017.08.004>
- [4] K. Auepattana-Aumrung, D. Crespy, *Chemical Engineering Journal*, 452 (2023) 139055; <https://doi.org/10.1016/j.cej.2022.139055>
- [5] B. Chen, Q. Wu, et al., *Chemical Engineering Journal*, 379 (2020) 122323; <https://doi.org/10.1016/j.cej.2019.122323>
- [6] Y. Huang, L. Deng, et al., *ACS Appl*, 10 (2018) 23369-23379; <https://doi.org/10.1021/acsami.8b06985>
- [7] Z. Hu, D. Zhang, et al., *Macromolecules*, 51 (2018) 5294-5303; <https://doi.org/10.1021/acs.macromol.8b01124>
- [8] F. Varela, M.Y.J. Tan, et al., *Electrochimica Acta*, 186 (2015) 377-390; <https://doi.org/10.1016/j.electacta.2015.10.171>
- [9] H. Zheng, B. Zhang, et al., *Chemical Engineering Journal*, 452 (2023) 139043; <https://doi.org/10.1016/j.cej.2022.139043>
- [10] M. Finšgar, D. Čakara, *Applied Surface Science*, 606 (2022) 154843; <https://doi.org/10.1016/j.apsusc.2022.154843>
- [11] Y. He, W. Xu, et al., *RSC Adv*, 5 (2015) 90609-90620; <https://doi.org/10.1039/C5RA19296J>
- [12] H. Li, Y. Qiang, W. Zhao, S. Zhang, *Corrosion Science*, 191 (2021) 109715; <https://doi.org/10.1016/j.corsci.2021.109715>
- [13] C. Dong, M. Zhang, T. Xiang, L. Yang, et al., *J Mater Sci*, 53 (2018) 7793-7808; <https://doi.org/10.1007/s10853-018-2046-5>
- [14] Y. Ye, H. Chen, Y. Zou, Y. Ye, H. Zhao, *Corrosion Science*, 174 (2020) 108825; <https://doi.org/10.1016/j.corsci.2020.108825>
- [15] N. Keshmiri, P. Najmi, et al., *Journal of Cleaner Production*, 319 (2021) 128732; <https://doi.org/10.1016/j.jclepro.2021.128732>
- [16] M. Ramezanzadeh, B. Ramezanzadeh, M. Mahdavian, G. Bahlakeh, *Carbon*, 161 (2020) 231-251; <https://doi.org/10.1016/j.carbon.2020.01.082>
- [17] H.-C. Zhou, J. R. Long, O. M. Yaghi, *Chem. Rev*, 112 (2012) 673-674; <https://doi.org/10.1021/cr300014x>
- [18] T. Islamoglu, S. Goswami, et al., *Acc. Chem. Res*, 51 (2018) 212-212; <https://doi.org/10.1021/acs.accounts.7b00620>
- [19] H. Yan, X. Fan, et al., *Journal of Colloid and Interface Science*, 602 (2021) 131-145; <https://doi.org/10.1016/j.jcis.2021.06.004>
- [20] Y. Zhao, T. Xu, J.-H. Zhou, J.-M. Hu, *Chemical Engineering Journal*, 433 (2022) 134039; <https://doi.org/10.1016/j.cej.2021.134039>

- [21] N. Wang, Y. Zhang, J. Chen, J. Zhang, Q. Fang, *Progress in Organic Coatings*, 109 (2017) 126-134; <https://doi.org/10.1016/j.porgcoat.2017.04.024>
- [22] K.S. Park, Z. Ni, et al., *Proc. Natl. Acad. Sci. U.S.A.*, 103 (2006) 10186-10191; <https://doi.org/10.1073/pnas.0602439103>
- [23] G.A. Gamov, M.N. Zavalishin, V.A. Sharnin, *Spectrochimica Acta Part A: Molecular and Biomolecular Spectroscopy*, 206 (2019) 160-164; <https://doi.org/10.1016/j.saa.2018.08.009>
- [24] S. Kumaraguru, R. Pavulraj, S. Mohan, *Transactions of the IMF*, 95 (2017) 131-136; <https://doi.org/10.1080/00202967.2017.1283898>